ELSEVIER

Journal of Nuclear Materials 297 (2001) 153–160

journal of nuclear materials

www.elsevier.com/locate/jnucmat

Diffusion reactions in titanium/Inconel-600 system

R.V. Patil, G.B. Kale *, P.S. Gawde

Materials Science Division, Bhabha Atomic Research Centre, Mumbai 400 085, India

Received 28 March 2001; accepted 3 May 2001

Abstract

The interdiffusion reactions in the Ti/Inconel-600 system in the temperature range 973–1153 K have been investigated by employing both the optical metallography and the electron probe microanalysis techniques. At 973 K the reaction zone showed the presence of solid solution phases like Ni-based (Fe, Cr, Ti) phase and titanium-based solid solution α-Ti. The two intermetallic phases, viz. TiNi(Fe, Cr) and Ti_2Ni are also observed. At 1023 K the reaction zone shows the formation of the two intermetallic phases, viz. TiNi(Fe, Cr) and Ti_2Ni along with solid solution phases such as Ni-based (Fe, Cr, Ti) phase and titanium-based solid solution β-Ti. At still higher temperatures (1073–1153 K), however, along with the solid solution phases such as Ni-based (Fe, Cr, Ti) phase and titanium-based solid solution β-Ti only one intermetallic phase, $TiNi_3$ (Fe, Cr), is formed. The temperature dependence of the reaction constants, K, $m/s^{1/2}$, derived from the layer growth kinetics, can well be expressed as

for Ni-rich phase
$K = 3.06 \times 10^{-5} \exp(-262.16/RT), \quad m/s^{1/2}$
for $TiNi_3$(Fe, Cr)
$K = 3.49 \times 10^{-5} \exp(-240.96/RT), \quad m/s^{1/2}$
for β-Ti
$K = 1.25 \times 10^{-6} \exp(-983.80/RT), \quad m/s^{1/2}$.

Here activation energy is expressed in kJ/mol. The interdiffusion parameters and the diffusion paths have also been established by employing these data.

1. Introduction

The nickel-based super alloys (Ni–Cr–Fe) find extensive use in high temperature (>1100 K) applications in modern high-tech industries. Their superior strength and better structural stability at elevated temperatures are complemented by hot corrosion resistant properties. These alloys generally contain alloying elements like Al, Ti, etc. in substantial levels. The hardening of the matrix caused due to the precipitation of coherent ordered fcc γ′-phase, Ni_3 Ti (Al), contributes to the strength of the alloy. Although under hot-corrosion conditions Ti is more favoured over Al, excess titanium may give rise to the formation of non-coherent-phase (Ti_3Ni). Similarly with prolonged exposure to high temperatures, the incoherent secondary σ-laves or μ-phases may form. The presence of these non-coherent phases is detrimental to the structural as well as metallurgical stability of the alloy. The interdiffusion at ambient temperatures plays a major role in controlling the mechanical properties of the component while in service. Therefore the study of diffusion reaction mechanism and the layer growth kinetics of intermetallic compounds in diffusion bonded couples are of both academic and technological importance. The interdiffusion studies in the binary Ti–Ni [1], Ti–Fe [2] and Ti–Al [3] systems have been reported earlier in the literature. The formation of various phases and intermetallic compounds with a wide range of layer growth kinetics have been observed in the investigations of the diffusion zones of these couples. To our knowledge no interdiffusion studies on Inconel with Ti have been reported so far in the literature. This paper reports

* Corresponding author.
E-mail address: gbkale@apsara.barc.ernet.in (G.B. Kale).

0022-3115/01/$ - see front matter
PII: S0022-3115(01)00613-4

the systematic metallographic and electron probe microanalytical investigations on the interdiffusion reactions in the Ti/Inconel-600 system in the temperature range between 973 and 1153 K.

2. Experimental

2.1. Material selection and preparation of diffusion couples

The coarse grained rectangular pieces of pure (>98.99%) Ti and commercial grade Inconel-600 (76%Ni, 16%Cr and 8%Fe), approximately 10 mm × 10 mm × 8 mm in dimensions are employed in making butt-type diffusion couples. After grinding on successive grade emery papers, these pieces are finally polished on a wheel lapped with 1 μm alumina powder suspended in water to give plane surfaces with good metallographic finish. The diffusion couples are made by putting the polished surfaces together under pressure (~6.89 MPa) in a die and heating them at a temperature of 973 K for 30 min in a vacuum (>10^{-5} mm of Hg). These couples are sealed in the quartz capsules filled with helium (~101 kPa) and diffusion annealed in a preheated resistance furnace in the temperature range between 973 and 1153 K for the duration of 100 h. The temperature of the furnace is controlled within ±1 K.

2.2. EPMA and metallographic analysis

The diffusion annealed couples are cut across the interface parallel to the diffusion direction and are prepared for metallography and electron probe microanalysis. The specimens are ground on a successive grade emery papers and polished on a wheel lapped with 1 μm diamond/0.5 μm alumina slurry to get good metallographic finish.

2.2.1. Elemental analysis by EPMA

The polished and unetched diffusion couples are analysed to get concentration penetration profiles of various elements by employing the CAMEBAX electron probe micro-analyser (EPMA) in a wavelength dispersive mode. The EPMA is operated with a stabilised beam current of 100 nA at 15 kV accelerating voltage. The intensities of FeKα, NiKα, CrKα, and TiKα radiations are recorded by diffracting respective characteristic X-rays with the help of a LiF crystal. The raw intensity data are generated by scanning the couple across the diffusion zone. The X-ray intensity ratios (*k*-ratios) are derived by dividing the raw intensity values by the intensity obtained from the respective pure metal standards. These *k*-ratios are corrected for atomic number (Z), atomic absorption (A) and fluorescence (F) effects to get the true compositions by using standard ZAF correction software. Depending on the width of the diffusion zone, the measurements are carried out in the pre-chosen steps.

2.2.2. The optical metallography

Metallographic techniques are used in determining the number of phases formed as a function of temperature. The polished surfaces are etched by using (HF: HNO_3:Glycerol::1:1:2) etchant to reveal the microstructure of the reacted diffusion zone after electroetching the Inconel side of the couple by 1 M oxalic acid solution with a current density of 1 A/cm^2. The layer thickness measurements are carried out by using both a calibrated Fehller eye piece and the EPMA profiles.

3. Diffusion data analysis

In a ternary metallic system with limited terminal solid solubility, intermediate phases do form in the diffusion zone. Jan et al. [4] have described the unidirectional growth of *n*-phases in a semi-infinite, ternary diffusion couple. They have derived the interdiffusion coefficients in these phases from the knowledge of the layer growth kinetics and the corresponding concentration profiles across the phases in the diffusion zone. Fig. 1 shows the schematic concentration profile across the diffusion zone for the elements 1 and 2 in a 1–2–3 ternary system having α and γ as solid solutions and β as an intermediate phase. The movement of an interface and hence the growth of an intermediate phase is governed by the net mass transfer across the interface [5,6]. Therefore, the growth of β-phase is controlled by the net diffusion flux of the element across the α/β and β/γ interfaces. The migration rate of the interface ($\xi^{\alpha,\beta}$) will depend upon the difference in the flux ($J^{\alpha,\beta} - J^{\beta}$), and

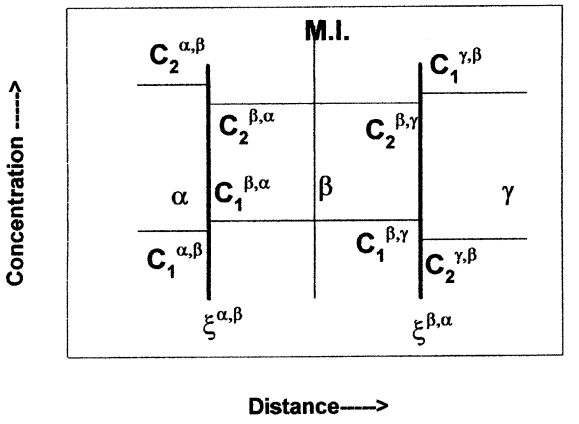

Fig. 1. The schematic concentration profile and the position of interfaces across the intermediate β-phase in 1,2,3 ternary couple.

the concentration gap $(C^{\alpha,\beta} - C^{\beta,\alpha})$ at the interface. If the elemental concentrations of 1 and 2 are taken as independent variables, then the rate of migration of an interface can be written as

$$\mathrm{d}(\xi^{\alpha,\beta})/\mathrm{d}t = [(J_i^{\alpha,\beta} - J_i^{\beta,\alpha})/(C_i^{\alpha,\beta} - C_i^{\beta,\alpha})] \quad (1)$$

with $i = 1, 2$. The diffusion fluxes, J_is in α and β phases are related to the ternary diffusion coefficients, D_{i1}s and D_{i2}s and can be expressed in terms of the Fick's law as

$$J_i^{\alpha,\beta} = -[(D_{il}^{\alpha}(\partial c_i/\partial x)^{\alpha,\beta} + D_{i2}^{\alpha}(\partial c_i/\partial x)^{\alpha,\beta}], \quad (2)$$

$$J_i^{\beta,\alpha} = -[(D_{il}^{\beta}(\partial c_i/\partial x)^{\beta,\alpha} + D_{i2}^{\beta}(\partial c_i/\partial x)^{\beta,\alpha}], \quad (3)$$

where the concentration gradients $(\partial c_i/\partial x)$ are taken at the respective interfaces.

Substituting Eqs. (2) and (3) in Eq. (1)

$$\begin{aligned}\mathrm{d}(\xi^{\alpha,\beta})/\mathrm{d}t = & -\{[D_{il}^{\alpha}(\partial c_i/\partial x)^{\alpha,\beta} + D_{i2}^{\alpha}(\partial c_i/\partial x)^{\alpha,\beta}] \\ & - [D_{il}^{\beta}(\partial c_i/\partial x)^{\beta,\alpha} + D_{i2}^{\beta}(\partial c_i/\partial x)^{\beta,\alpha}]\}/ \\ & (C_i^{\alpha,\beta} - C_i^{\beta,\alpha}). \end{aligned} \quad (4)$$

Now, on the application of the Boltzmann transformation [7,8], $\lambda = x/\sqrt{t}$ and since the concentration at the interface remains constant, $\mathrm{d}c/\mathrm{d}\lambda$ at the interface is also constant. Further assuming that all D_s are constant, Eq. (4) can be written as

$$\begin{aligned}\mathrm{d}(\xi^{\alpha,\beta})/\mathrm{d}t = & -[(D_{il}^{\alpha}\eta_1^{\alpha,\beta} + D_{i2}^{\alpha}\eta_2^{\alpha,\beta}) \\ & - (D_{il}^{\beta}\eta_1^{\beta,\alpha} + D_{i2}^{\beta}\eta_2^{\beta,\alpha})]/(C_i^{\alpha,\beta} - C_i^{\beta,\alpha})\sqrt{t}, \end{aligned} \quad (5)$$

where $\eta_1 = \sqrt{t}\partial c_1/\partial x$ and $\eta_2 = \sqrt{t}\partial c_2/\partial x$. Eq. (5) on integration gives

$$\begin{aligned}\xi^{\alpha,\beta} = & -2\sqrt{t}\{(D_{il}^{\alpha}\eta_1^{\alpha,\beta} + D_{i2}^{\alpha}\eta_2^{\alpha,\beta}) \\ & - (D_{il}^{\beta}\eta_1^{\beta,\alpha} + D_{i2}^{\beta}\eta_2^{\beta,\alpha})\}/(C_i^{\alpha,\beta} - C_i^{\beta,\alpha}). \end{aligned} \quad (6)$$

Fig. 2 shows the formation of an intermediate phase 'm' which is bounded by $(m-1, m)$ and $(m, m+1)$ interfaces in a multiphase ternary diffusion couple. For the mth layer, therefore, Eq. (6) can be written as

$$\begin{aligned}\xi^{m-1,m} = & -2\sqrt{t}\{(D_{i1}^{m-1}\eta_1^{m-1,m} + D_{i2}^{m-1}\eta_2^{m-1,m}) \\ & - (D_{il}^{m}\eta_1^{m,m-1} + D_{i2}^{m}\eta_2^{m,m-1})\}/(C_i^{m-1,m} - C_i^{m,m-1}). \end{aligned} \quad (7)$$

The migration of interface $\xi^{m,m-1}$, can similarly, be expressed in terms of diffusivities and the concentration gradients at the respective interfaces.

Now for the ease of calculations one can further assume the absence of mutual interactions between the diffusing species so that the cross-diffusion coefficients $(D_{12}, D_{21}$, etc.) are zero. In such conditions the position of interface, $\xi^{m-1,m}$ in terms of element 1 (or element 2) can be written as

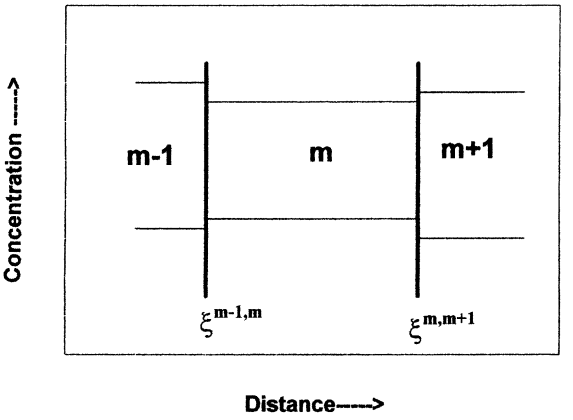

Fig. 2. Schematic formation of phase 'm' bounded by $(m-1, m)$ and $(m, m+1)$ interfaces in multiphase ternary diffusion couple.

$$\xi^{m-1,m} = -2\sqrt{t}(D_{11}^{m-1}\eta_1^{m-1,m} + D_{11}^{m}\eta_1^{m,m-1})/(C_1^{m-1,m} - C_1^{m,m-1}) \quad (8)$$

or

$$\xi^{m-1,m} = -2\sqrt{t}(D_{22}^{m-1}\eta_2^{m-1,m} + D_{22}^{m}\eta_2^{m,m-1})/(C_2^{m-1,m} - C_2^{m,m-1}). \quad (9)$$

By employing Eq. (8) or (9), the interdiffusion coefficients can be obtained in multiphase ternary diffusion system. While the values of ηs are derived from the knowledge of the rate growth kinetics (Eq. (10)), the $(C_i^{m-1,m} - C_i^{m,m-1})$ is read directly from the respective concentration profiles. The value of $\xi^{m-1,m}$ is taken as the displacement from the Matano interface [7,8].

4. Results and discussion

4.1. Metallographic and EPMA investigations

Figs. 3–8 show the optical micrographs of the reaction zones and the corresponding concentration profiles from the diffusion couples annealed in the temperature range between 973 and 1153 K for the duration of 100 h.

Fig. 3 shows the micrograph of the couple annealed at 973 K. It clearly shows the formation of nickel-rich solid solution Ni–(Fe, Cr, Ti) phase, which appears as the dark region (marked 'a') in the micrograph. The formation of two intermetallic phases, viz. TiNi(Fe, Cr) (marked 'b') and Ti_2Ni (marked 'c') is also revealed in the micrograph. The concentration profiles, established with the help of EPMA (Fig. 4) also indicate the formation of these phases. Additionally it also shows the formation of metastable α-Ti solid solution containing 5–25 at.%Ni. This phase could not be revealed by metallography.

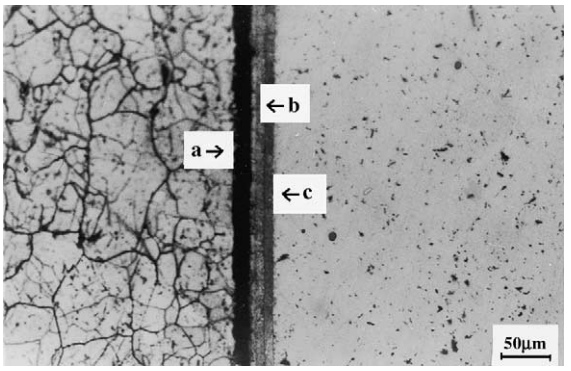

Fig. 3. Micrograph of the diffusion zone of the couple annealed at 973 K for 100 h in Ti/Inconel-600 system: (a) Ni–(Fe, Cr, Ti); (b) TiNi(Fe, Cr); (c) Ti_2Ni.

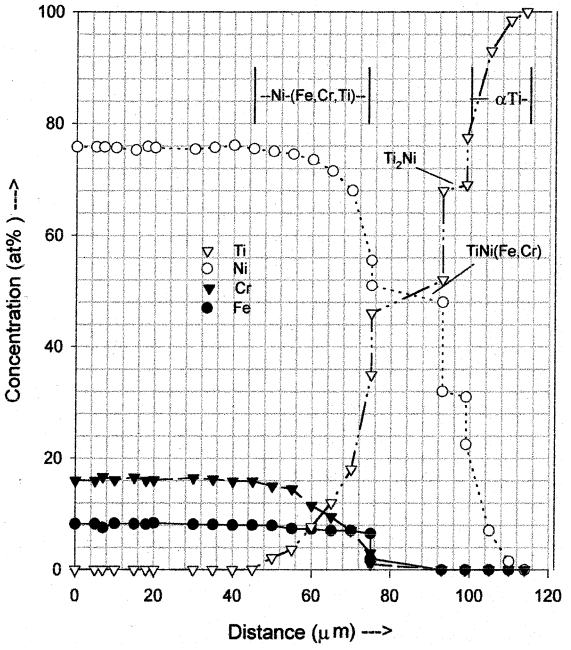

Fig. 4. The concentration penetration profiles across the diffusion zone for the couple annealed at 973 K for 100 h in Ti/Inconel-600 system.

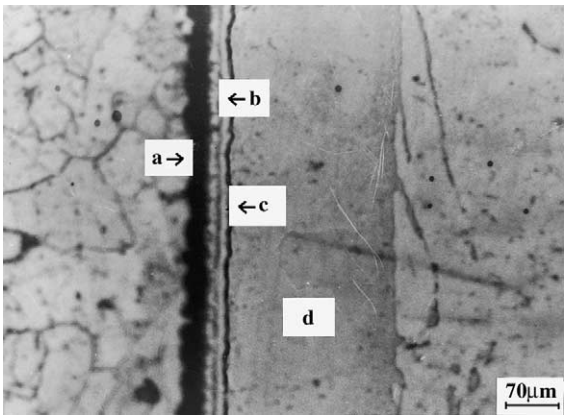

Fig. 5. Micrograph of the diffusion zone of the couple annealed at 1023 K for 100 h in Ti/Inconel-600 system: (a) Ni–(Fe, Cr, Ti); (b) TiNi(Fe, Cr); (c) Ti_2Ni; (d) β-Ti.

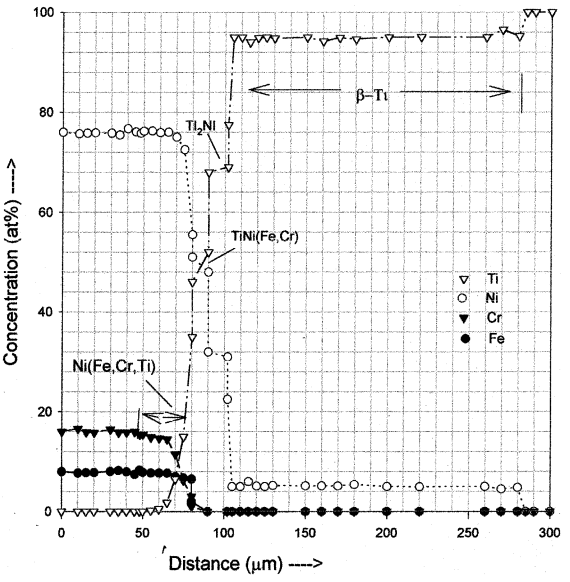

Fig. 6. The concentration penetration profiles across the diffusion zone for the couple annealed at 1023 K for 100 h in Ti/Inconel-600 system.

Fig. 5 shows the micrograph for the couple annealed at 1023 K. It indicates the formation of nickel rich solid solution (marked as 'a'), β-Ti with 3–5 at.%Ni, (marked as 'd') along with the intermetallic compounds, TiNi(Fe, Cr) (marked as 'b') and Ti_2Ni (marked as 'c'). The EPMA results (Fig. 6) also confirm the formation of these compounds along with the solid solution phases in the diffusion zone.

Fig. 7 shows the micrograph of the couple annealed at 1073 K. It shows both the nickel rich (marked as 'a') and titanium rich (marked as 'c') solid solutions along with only one intermetallic compound, viz. $TiNi_3$ (Fe, Cr) (marked as 'b'). The corresponding EPMA profiles (Fig. 8) confirm the results. At still higher temperatures (1133–1153 K), the morphology of the diffusion zone is very similar to that observed at 1073 K except for the difference in the phase width and in the width of diffusion zones.

It is noticed that although very little or no Fe/Cr has diffused towards the titanium side of the couple, the substantial quantity (3–5 at.%) of Ni has diffused across

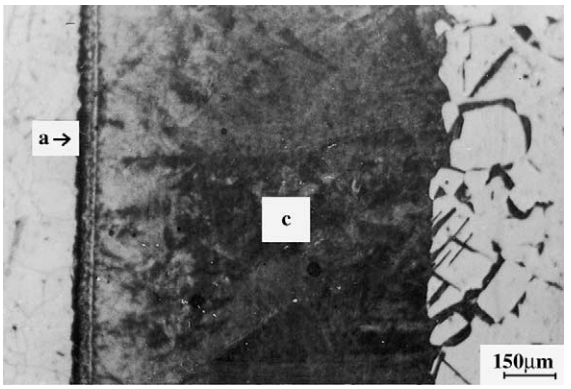

Fig. 7. The micrograph of diffusion zone for the couple annealed at 1073 K for 100 h in Ti/Inconel-600 system: (a) Ni–(Fe, Cr, Ti); (b) $TiNi_3$ (Fe, Cr); (c) β-Ti.

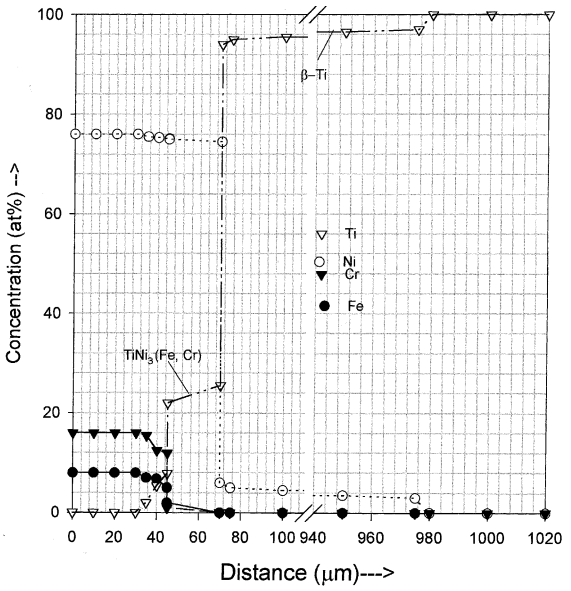

Fig. 8. The concentration penetration profiles across the diffusion zone for the couple annealed at 1073 K for 100 h in Ti/Inconel-600 system.

the zone to form β-Ti solid solution. Contrary to the present investigations, the earlier studies on titanium/stainless steel system [9] showed that iron from stainless steel has diffused to form β-Ti solid solution with Fe. The difference in the nature of the diffusion reaction may be due to the fact that when the diffusivities are comparable ($D_{Fe}/D_{Ni} \approx 1$) the flux of a specie depends upon the concentration gradient. The latter in turn depends upon the difference in the initial composition of the components of the couple. Hence, in Ti/Inconel-600 system, nickel being a major component in Inconel-600, initial difference in nickel concentration is more as compare to iron and chromium. This must have caused the formation of nickel-based solid solutions and compounds in the reaction zone of this system.

4.2. Diffusion paths and the intermetallic phases in the diffusion zone

The nature of the diffusion path in the single phase region of a ternary system is generally S-shaped. The extent of deviation from linearity depends upon the relative magnitudes of the diffusion coefficient and the activity of the diffusing species. The diffusion path moves along the constant concentration lines of the slowest moving specie [10]. Further, superimposing the diffusion paths on the isotherm of the ternary system, one can predict the formation of intermetallic phases during the interdiffusion reaction. Similarly, the isotherm can also be constructed from the knowledge of both interdiffusion reactions and the diffusion paths representing the diffusion couple. The Ti/Inconel system has four major diffusing species, viz. Ti, Ni, Fe and Cr. It is very difficult to draw and illustrate the diffusion paths in a quaternary system on two-dimensional Cartesian co-ordinates. In the present studies, the concentration of Cr remains more or less constant (rather decreases very slowly) on the Inconel side of the couple. In addition, the intermetallic phases TiNi (Fe, Cr) and $TiNi_3$ (Fe, Cr) have a very low Cr content (<1 at.%). After taking into account all these observations we have attempted to construct an isotherm based on Ti–Fe–Ni as a ternary system by converting chromium into an equivalent iron content. The effect of presence of chromium on the diffusion reaction, if any is also ignored.

The concentration profiles obtained from the diffusion zones of the couples annealed in the temperature range 973–1153 K are transformed on to the isotherm to represent the ternary diffusion paths. The concentrations of the phase boundaries are taken from the Ti–Ni–Fe isotherm at 1173 K available in the literature [11]. Fig. 9 shows a typical diffusion path drawn by employing the present diffusion data at 973 K. It follows the line A–B in the nickel rich solid solution, C–D in TiNi(Fe), E–F in Ti_2Ni and G–H in Ti-rich solid solution region. It must be mentioned here that the isotherm at 973 K reported earlier [11] does not show the formation of α-Ti solid solution and the intermetallic phases TiNi(Fe) and Ti_2Ni. The diffusion path at 1023 K is similar to one at 973 K. These diffusion paths show the presence of Ti_2Ni and $TiNi_3$ (Fe) intermetallic phases along with the broad region of nickel-rich solid solution. Similar diffusion paths have also been established for higher temperatures. These paths passed through the regions such as nickel rich solid solution, $TiNi_3$ (Fe) phase and a β-Ti solid solution as depicted in the isotherm at 1173 K.

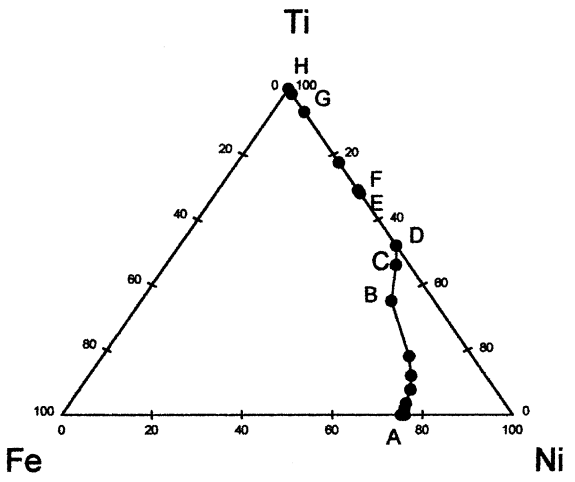

Fig. 9. Diffusion path through various phases (A–B in Ni-based solid solution, C–D in TiNi(Fe), E–F in $NiTi_2$ and G–H in Ti-based solid solution) for a couple annealed at 973 K for 100 h.

4.3. The layer growth kinetics

The layer growth thickness (X) of the various intermetallic phases in the diffusion zone of the couples annealed can be represented by the relation

$$X = Kt^{1/n}, \tag{10}$$

where K is the reaction constant, n, the reaction index and t is time of anneal. The reaction constant K follows the temperature dependence given by the equation

$$K = K_0 \exp(-Q_p/RT). \tag{11}$$

The layer growth thickness (X) of the various intermetallic phases in the diffusion zone of the couples annealed isochronally at various temperatures can be obtained by combining Eqs. (10) and (11) and can be represented by the relation

$$X = K_0 \exp(-Q_p/RT)t^{1/n}, \tag{12}$$

where K_0 is pre-exponential factor and Q_p is the activation energy for the phase growth.

The layer growth data for various phases (Table 1) show the linear relationship with reciprocal absolute temperatures (Fig. 10). By assuming $n = 2$, the values of Q_p (kJ/mol) and K_0 ($m/s^{1/2}$) for various phases are evaluated. The temperature dependence of reaction constants for various phases is expressed as

for Ni-rich solid solution phase,

$$K = 3.06 \times 10^{-5} \exp(-262.16/RT), \quad m/s^{1/2} \tag{13}$$

for $TiNi_3$ (Fe, Cr),

$$K = 3.49 \times 10^{-5} \exp(-240.96/RT), \quad m/s^{1/2} \tag{14}$$

for β-Ti,

$$K = 1.25 \times 10^{-6} \exp(-983.80/RT), \quad m/s^{1/2}. \tag{15}$$

These parabolic rate constants are employed in solving Eqs. (8) or (9) to obtain diffusion coefficient values in the respective phases. As the limited data are available for

Table 1
Interdiffusion coefficients and the phase widths of various intermetallic phases at various temperatures in Ti/Inconel system annealed for 100 h

Temperature (K)	Phase grown	Phase thickness ($m \times 10^6$)	Interdiffusion coefficients	
			D^{Fe}_{NiNi} (m^2/s)	D^{Fe}_{TiTi} (m^2/s)
973	Ni-rich solid solution	15	8.78×10^{-17}	1.28×10^{-16}
	TiNi (Fe, Cr)	18	7.92×10^{-16}	6.75×10^{-16}
	Ti_2Ni	6	6.60×10^{-16}	8.22×10^{-16}
	α-Ti	15	2.78×10^{-19}	7.40×10^{-18}
1023	Ni-rich solid solution	20	4.70×10^{-16}	4.40×10^{-16}
	TiNi (Fe, Cr)	10	4.90×10^{-15}	2.40×10^{-15}
	Ti_2Ni	12	1.44×10^{-14}	1.44×10^{-14}
	β-Ti	178	1.05×10^{-12}	1.05×10^{-12}
1073	Ni-rich solid solution	15	1.77×10^{-13}	4.97×10^{-14}
	$TiNi_3$ (Fe, Cr)	25	1.37×10^{-13}	8.75×10^{-15}
	β-Ti	930	1.16×10^{-13}	1.16×10^{-13}
1113	Ni-rich solid solution	15	2.83×10^{-13}	1.40×10^{-14}
	$TiNi_3$ (Fe, Cr)	30	2.53×10^{-13}	4.22×10^{-13}
	β-Ti	1580	4.83×10^{-13}	4.80×10^{-13}
1153	Ni-rich solid solution	20	2.42×10^{-12}	1.03×10^{-13}
	$TiNi_3$ (Fe, Cr)	40	2.94×10^{-12}	4.90×10^{-13}
	β-Ti	6370	7.66×10^{-12}	7.66×10^{-12}

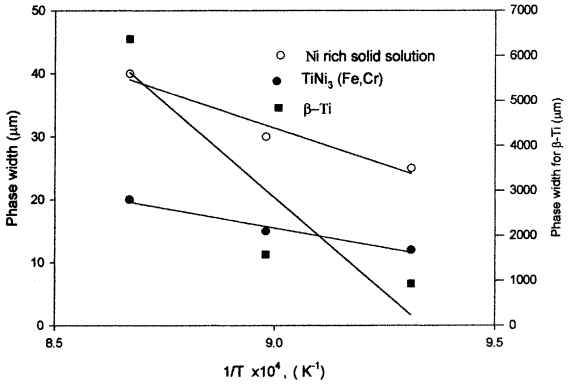

Fig. 10. The temperature dependence of layer thickness of various phases in Ti/Inconel-600 system.

TiNi(Fe, Cr) and Ti_2Ni compounds, the reaction constants are not evaluated in these compounds.

4.4. The interdiffusion coefficients

As discussed earlier (Section 3) the diffusivity values D^{Fe}_{NiNi}, D^{Fe}_{TiTi}, etc. are evaluated by employing Eqs. (8) or (9). While the data for η values for various phases are obtained from the temperature dependence of $K(=dx/\sqrt{t})$, the ξ-values (i.e. the positions from Matano-interfaces) and the concentrations at the interfaces, are read directly from the respective concentration profiles. The concentration profiles in the temperature range 1023–1153 K do not show measurable penetration of Fe into the titanium side of the couple indicating the flux of the diffusing species in titanium to be negligibly small. Hence, D^{Fe}_{NiNi} and D^{Fe}_{TiTi} values in Ti are taken as zero while evaluating the diffusivities in the adjoining phases in the diffusion zone. In the case of α-Ti solid solution, formed at 973 K, however, these values are taken as the respective tracer diffusivities of Ni [12] and Ti [13] in α-Ti. The diffusion coefficients in various phases appeared in the diffusion zone of the couples have been evaluated and are listed in Table 1.

As the ternary diffusion data in Ti–Ni–Fe are not available in literature for comparison, we have adopted the procedure established by Shunk and Tool [14] to determine the diffusivity values in the limiting concentrations at the arms of the 1–2–3 ternary isotherm. That is to say that when the solute concentration of the third element becomes zero then the system becomes binary and hence the values of ternary diffusion coefficients can be compared with binary interdiffusion coefficients. In the case of TiNi(Fe, Cr), $TiNi_3$ (Fe, Cr) and β-Ti, have negligible concentration of Fe. Hence the ternary diffusion coefficients D^{Fe}_{NiNi} in these phases should be comparable to that of binary Ti–Ni system. We have calculated such interdiffusion coefficient values for the limiting concentration of iron and they are listed in Table 2 along with the available binary Ti–Ni interdiffusion coefficient values [1]. It can be seen that D^{Fe}_{NiNi} in TiNi(Fe, Cr) and β-Ti are comparable to binary Ti–Ni interdiffusion coefficient values. The binary interdiffusion coefficients in $TiNi_3$ (Fe, Cr) are not available and hence can not be compared.

The values of log of ternary diffusion coefficients are plotted against the reciprocal of the diffusion annealing temperature to establish the temperature dependence in Fig. 11. The values of the interdiffusion parameters, viz.

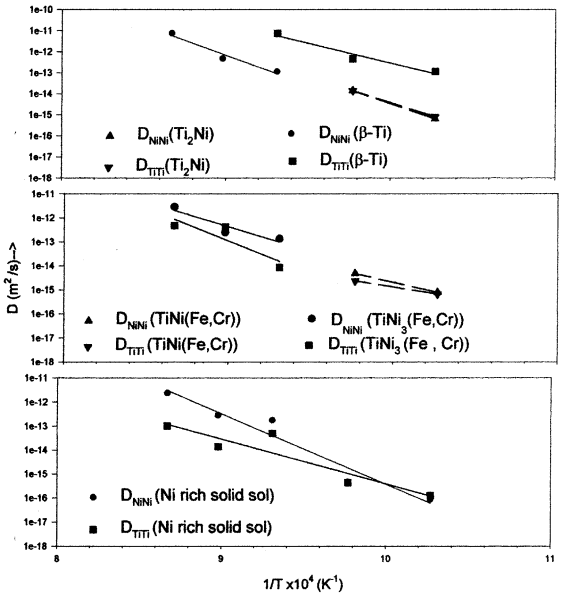

Fig. 11. The temperature dependence of diffusion coefficients in various phases in Ti/Inconel-600 system.

Table 2
Comparison of ternary diffusion coefficient with binary diffusion coefficient in Ti/Inconel system

Temperature (K)	Phase	D^{Fe}_{NiNi} (m^2/s)	D (Ti–Ni) (m^2/s)	References
973	TiNi(Fe, Cr)	7.92×10^{-16}	5.1×10^{-15}	[1]
1023	TiNi(Fe, Cr)	4.9×10^{-15}	8.5×10^{-15}	[1]
1073	β-Ti	1.16×10^{-13}	6.21×10^{-13}	[12]
1113	β-Ti	4.83×10^{-13}	2.5×10^{-12}	[1]
1153	β-Ti	7.66×10^{-12}	3.2×10^{-12}	[1]

Table 3
Interdiffusion parameters for various phases in Ti/Inconel system

Phase	Diffusion coeff.	D_0 (m^2/s)	Q (kJ/mol)
Ni-rich solid solution	D^{Fe}_{NiNi}	1.02×10^{14}	207.37
	D^{Fe}_{TiTi}	1.97×10^{03}	155.42
$TiNi_3$ (Fe, Cr)	D^{Fe}_{NiNi}	1.75×10^{06}	171.84
	D^{Fe}_{TiTi}	7.27×10^{11}	229.20
β-Ti	D^{Fe}_{NiNi}	2.17×10^{13}	235.52
	D^{Fe}_{TiTi}	2.12×10^{06}	156.79

pre-exponential factor (D_0) and activation energy (Q) for various diffusion coefficient values are computed by using linear regression and are tabulated in Table 3. As mentioned earlier the values of activation energies for D^{Fe}_{NiNi} in TiNi(Fe,Cr), $TiNi_3$ (Fe,Cr), Ti_2Ni and β-Ti should be comparable to those of activation energies for binary diffusion in the respective phases. The activation energy value (156.79 kJ) for D^{Fe}_{NiNi} in β-Ti is comparable with the value of 141.00 kJ reported for binary Ti–Ni interdiffusion [1]. The activation energy for other phases could not be compared due to the non-availability of data in literature.

5. Summary

The experimental results on the reaction diffusion in Ti/Inconel-600 system annealed in the temperature range 973–1153 K are summarised below:

1. In Ti/Inconel-600 system, two intermetallic phases, viz. TiNi (Fe, Cr) and Ti_2Ni along with the solid solutions, viz. Ni (Fe, Cr, Ti), α-Ti and β-Ti form below 1073 K.
2. Above 1073 K phases formed at low temperature disappear and only one intermetallic phase, $TiNi_3$ (Fe, Cr) is found to grow along with the solid solutions.
3. The temperature dependence of the reaction constants, K for various phases can be expressed by the following Arrhenius relationships:

   for Ni-rich solid solution phase,

   $$K = 3.06 \times 10^{-5} \exp(-262.16/RT), \quad m/s^{1/2}$$

   for $TiNi_3$ (Fe, Cr),

   $$K = 3.49 \times 10^{-5} \exp(-240.96/RT), \quad m/s^{1/2}$$

   for β-Ti,

   $$K = 1.25 \times 10^{-6} \exp(-983.80/RT), \quad m/s^{1/2}.$$

4. The direct diffusion coefficients D^{Fe}_{NiNi} and D^{Fe}_{TiTi} are in the range 10^{-17}–10^{-12} m^2/s in Ni-rich solid solution and in the range 10^{-13}–10^{-12} m^2/s in Ti-based solid solution. The values of D^{Fe}_{NiNi} and D^{Fe}_{TiTi} in intermetallic phases TiNi(Fe, Cr) and Ti2Ni are in the range 10^{-16}–10^{-15} m^2s and 10^{-16}–10^{-14} m^2/s, respectively. Similar values for intermetallic phase $TiNi_3$ (Fe, Cr) are in the range 10^{-13}–10^{-12} m^2/s.
5. The values of ternary diffusion coefficients in limiting concentrations of Fe are comparable to those for binary diffusion coefficients in Ti–Ni System.
6. The temperature dependence of ternary diffusion coefficients can be described by using the Arrhenius relationship. The values of pre-exponential factor D_0 and activation energy Q for β-Ti solid solution are comparable to those for binary diffusion in Ti–Ni System.

Acknowledgements

The authors are grateful to Dr P. Mukhopadhyaya, Head Physical Metallurgy Section and Dr S. Banerjee, Director, Materials Group, BARC for their keen interest in the work.

References

[1] G.F. Bastin, G.D. Rieck, Metall. Trans. 5 (1974) 1817 and 1827.
[2] K. Hirano, Y. Iposhi, J. Jpn. Inst. Met. 39 (1968) 815.
[3] F.J.J. van Loo, G.D. Rieck, Acta. Metall. 21 (1973) 61 and 73.
[4] C.-H. Jan, D. Swanson, X.-Y. Zheng, J.-C. Lin, Y.A. Chang, Acta. Metall. 39 (1991) 303.
[5] W. Jost, Diffusion in Solids, Liquids and Gases, 2nd Ed., Academic Press, New York, 1960, p. 68.
[6] J. Philibert, Atom Movements: Diffusion and Mass Transport in Solids, translated by S.J. Rothman, Les Editions de Physique, les Ulis, France 1991, p. 303.
[7] L. Boltzmann, Ann. Phys. 53 (1894) 595.
[8] C. Matano, Jpn. J. Phys. 8 (1930) 109.
[9] G.B. Kale, R.V. Patil, P.S. Gawde, J. Nucl. Mater. 257 (1999) 44.
[10] A. Guy, V. Levory, T.B. Lindemer, Trans. Am. Soc. Met. 59 (1966) 517.
[11] P. Villars, A. Prince, H. Okamata (Eds.), HandBook of Ternary Alloy Phase Diagrams, vol. 7, ASM, Metals Park, OH, p. 10655.
[12] L.S. Castlemann, Metall. Trans. 14 (1983) 45.
[13] J.R. Manning, Metall. Trans. 1 (1970) 499.
[14] F. Shunk, H.L. Tool, J. Phys. Chem. 67 (1963) 540.